Cyclic Metalloporphyrin Trimers: ^{1}H NMR Identification of Trimeric Heterometallic (Iron(III), Gallium(III), Manganese(III)) 2-Hydroxy-5,10,15,20-tetraphenylporphyrins and X-ray Crystal Structure of the Iron(III) 2-Hydroxy-5,10,15,20-tetra-*p*-tolylporphyrin Trimer[1]

Jacek Wojaczyński,[†] Lechosław Latos-Grażyński,*[,†] Marilyn M. Olmstead,[‡] and Alan L. Balch[‡]

Departments of Chemistry, University of Wrocław, 14 F. Joliot-Curie St., Wrocław 50 383, Poland, and University of California, Davis, California 95616

Received February 26, 1997[⊗]

Oligomerization of a mixture of monomeric iron(III) 2-hydroxy-5,10,15,20-tetraphenylporphyrin, (2-OH-TPP)-Fe^{III}Cl, manganese(III) 2-hydroxy-5,10,15,20-tetraphenylporphyrin, (2-OH-TPP)Mn^{III}Cl, and gallium(III) 2-hydroxy-5,10,15,20-tetraphenylporphyrin, (2-OH-TPP)Ga^{III}Cl, complexes affords the series of heterometallic cyclic trimeric species of the general formula $\{[(2\text{-O-TPP})Ga^{III}]_n[(2\text{-O-TPP})Fe^{III}]_{3-n}\}$, $\{[(2\text{-O-TPP})Ga^{III}]_n[(2\text{-O-TPP})Mn^{III}]_{3-n}\}$, and $\{[(2\text{-O-TPP})Fe^{III}]_n[(2\text{-O-TPP})Mn^{III}]_{3-n}\}$ ($n = 0-3$). The ^{1}H NMR spectroscopic and mass spectrometric investigations indicate that these compounds have a head-to-tail cyclic trimeric structure. In the ^{1}H NMR spectra the interactions between paramagnetic, weakly coupled centers are reflected by marked variations of chemical shifts and line widths of pyrrole resonances. The characteristic upfield positions of the 3-H pyrrole resonances are diagnostic for the trimeric motifs. The structure of the prototypical molecule, $[(2\text{-O-TTP})Fe^{III}]_3$, has been determined by X-ray crystallography. $[(2\text{-O-TTP})Fe^{III}]_3 \cdot 3n$-octane crystallizes in the monoclinic space group $P2_1/n$ with $a = 16.729(6)$ Å, $b = 43.671(13)$ Å, $c = 19.564(7)$ Å, $\beta = 105.83(3)°$, and $Z = 4$ at 130 K. The refinement of 1612 parameters and 5072 reflections yields $R_1 = 0.089$ and w$R_2 = 0.1848$. The trimeric iron(III) complex has a head-to-tail cyclic arrangement with the pyrrolic alkoxide groups forming bridges from one macrocycle to the metal in adjacent macrocycle. The three iron(III) porphyrin subunits are not equivalent but have typical geometry for high-spin five-coordinate iron(III) porphyrin complexes. The porphyrin skeleton of $[(2\text{-O-TTP})Fe^{III}]_3$ is expected to be representative of the structures of the homometallic and heterometallic trimeric complexes of 2-hydroxytetraarylporphyrin with M(III) ions.

Introduction

Metalloporphyrins which contain an additional binding center at the porphyrin periphery have been used as building blocks in a construction of large multiporphyrinic assemblies.[2,3] In these structures, the individual fragments are arranged by a self-assembly process and are joined by coordinate bonds between the metal ion and the peripheral functionality[2] or through multiple hydrogen bonding.[3] Frequently, the external coordination center is located at the *meso*-phenyl substituent of porphyrin.[2]

Recently we have synthesized and characterized unprecedented cyclic iron(III), gallium(III), and manganese(III) porphyrin trimers,[4−6] i.e. $[(2\text{-O-TPP})Fe^{III}]_3$, $[(2\text{-O-TPP})Ga^{III}]_3$, and $[(2\text{-O-TPP})Mn^{III}]_3$. These trimers were generated in a self-assembly process from monomeric iron(III) 2-hydroxy-5,10,15,20-tetraphenylporphyrin, gallium(III) 2-hydroxy-5,10,15,20-tetraphenylporphyrin, or manganese(III) 2-hydroxy-5,10,15,20-tetraphenylporphyrin, respectively. The crucial element of such a construction, i.e. 2-hydroxy-5,10,15,20-tetraphenylporphyrin,[7,8] represents features of a hybrid bifunctional ligand which contains two centers for coordination: the internal set of four pyrrolic nitrogen atoms and the external 2-O$^-$ group. In this particular case, the additional coordination center is located directly on the porphyrin ring. The coordination of a trivalent metal (rather than a divalent metal) by the porphyrin seems to be a

* Author to whom correspondence should be addressed.
† University of Wrocław.
‡ University of California.
⊗ Abstract published in *Advance ACS Abstracts,* August 15, 1997.

(1) Abbreviations: P, porphyrin dianion; TPP, 5,10,15,20-tetraphenylporphyrin dianion; TTP, 5,10,15,20-tetra-*p*-tolylporphyrin dianion; 2-OH-TPP, dianion of 2-hydroxy-5,10,15,20-tetraphenylporphyrin; 2-O-TPP, trianion of 2-hydroxy-5,10,15,20-tetraphenylporphyrin; 2-BzO-TPP, dianion of 2-(benzoyloxy)-5,10,15,20-tetraphenylporphyrin; OEB, octaethylbilindione trianion (biliverdin analog); FF, tetraanion of *N*,*N*′-bis(5-*o*-phenylene-10,15,20-triphenylporphyrin)urea.

(2) (a) Drain, C. M.; Lehn, J.-M. *J. Chem. Soc., Chem. Commun.* **1994,** 2313. (b) Kimura, A.; Funatsu, K.; Imamura, T.; Kido, H.; Sasaki, Y. *Chem. Lett.* **1995**, 207. (c) Fleisher, E. B.; Shachter, A. M. *Inorg. Chem.* **1991**, *30*, 3763. (d) Mackay, L. G.; Anderson, H. L.; Sanders, J. K. M. *J. Chem. Soc., Perkin Trans. 1* **1995**, 2269. (e) Anderson, S.; Anderson, H. L.; Bashall, A.; McPartlin, M.; Sanders, J. K. M. *Angew. Chem., Int. Ed. Engl.* **1995**, *34*, 1096. (f) Chi, X.; Guerin, A. J.; Haycock, R. A.; Hunter, C. A.; Sarson, L. D. *J. Chem. Soc., Chem. Commun.* **1995**, 2563. (g) Chi, X.; Guerin, A. J.; Haycock, R. A.; Hunter, C. A.; Sarson, L. D. *J. Chem. Soc., Chem. Commun.* **1995**, 2567. (h) Alessio, E.; Macchi, M.; Heath, S.; Marzilli, L. G. *Chem. Commun.* **1996**, 1411. (i) Chernook, A. V.; Rempel, U.; von Borczyskowski, C.; Shulga, A. M.; Zenkewich, E. I. *Chem. Phys. Lett.* **1996**, *254*, 229. (j) Sarson, L. D.; Ueda, K.; Takeuchi, M.; Shinkai, S. *Chem. Commun.* **1996**, 619. (k) Collin, J.-P.; Harriman, A.; Heitz, V.; Odobel, F.; Sauvage, J.-P. *Coord. Chem. Rev.* **1996**, *148*, 63.

(3) Drain, C. M.; Russel, K. C.; Lehn, J.-M. *Chem. Commun.* **1996**, 337.

(4) Wojaczyński, J.; Latos-Grażyński, L. *Inorg. Chem.* **1995**, *34*, 1044.

(5) Wojaczyński, J.; Latos-Grażyński, L. *Inorg. Chem.* **1995**, *34*, 1054.

(6) Wojaczyński, J.; Latos-Grażyński, L. *Inorg. Chem.* **1996**, *35*, 4812.

(7) (a) Crossley, M. J.; King, L. G.; Pyke, S. M. *Tetrahedron* **1987**, *43*, 4569. (b) Crossley, M. J.; Harding, M. M.; Sternhell, S. *J. Am. Chem. Soc.* **1986**, *108*, 3608. (c) Crossley, M. J.; Field, L. D.; Harding, M. M.; Sternhell, S. *J. Am. Chem. Soc.* **1987**, *109*, 2335. (d) Crossley, M. J.; Harding, M. M.; Sternhell, S. *J. Org. Chem.* **1988**, *53*, 1132. (e) Crossley, M. J.; Burn, P. L.; Langford, S. J.; Pyke, S. M.; Stark, A. G. *J. Chem. Soc., Chem. Commun.* **1991**, 1567.

(8) Callot, H. *Bull. Soc. Chim. Fr.* **1974**, 1492.

S0020-1669(97)00214-0 CCC: $14.00

prerequisite for the trimer formation. A series of divalent metal ions were reported to form only monomeric complexes with this ligand.[7]

The core of the trimer of the type $[(2\text{-O-TPP})M^{III}]_3$ can exist in two isomeric forms, **1** and **2**.

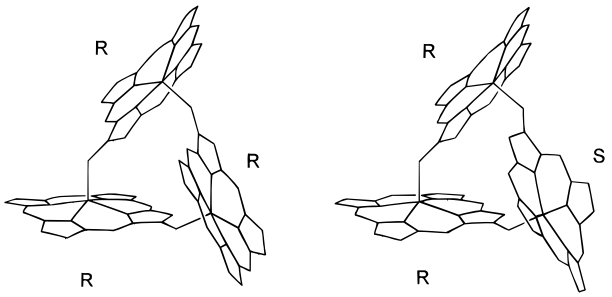

1 **2**

Within the trimer, each $(2\text{-O-TPP})M^{III}O-$ unit can exist as two optical antipodes.[4] The two enantiomers of (2-OH-TPP)-$Fe^{III}O$ form either a clockwise (*R*) or an anti-clockwise (*S*) arrangement of porphyrin β-substituents with respect to the iron(III)−axial ligand axis. In principle, during a random oligomerization an isomeric mixture of trimers will form that includes the two diastereometric pairs: *RRR*, *SSS* (with C_3 symmetry) and *RRS*, *SSR* (the pseudo-C_3 symmetry). Random oligomerization will produce a mixture that consists of 75% of the diastereometric pair *RRS*/*SSR* and 25% of the *RRR*/*SSS* pair.

Previous investigations on paramagnetic (iron(III), manganese(III)) and diamagnetic (gallium(III)) complexes established the ^{1}H NMR "fingerprints" for these cyclic trimers. Thus, in the case of $[(2\text{-O-TPP})Ga^{III}]_3$ there are three characteristic pyrrole resonances with upfield shifts at 1.82, 2.18, and 2.82 ppm (243 K).[5] The paramagnetic iron(III) trimer $[(2\text{-O-TPP})Fe^{III}]_3$ displays three 3-H signals which are strongly upfield shifted (−89.8, −94.7, and −99.3 ppm at 293 K).[4] The formation of the paramagnetic $[(2\text{-O-TPP})Mn^{III}]_3$ is characterized by the broad, unresolved 3-H pyrrole resonance with an upfield hyperfine shift (ca. −110 ppm, 293 K).[6] These and other ^{1}H NMR spctral features indicate that, after isolation, the trimers exist as the *RRS*/*SSR* pair.

Here we report the X-ray crystal structure of a prototypical cyclic trimer, $[(2\text{-O-TTP})Fe^{III}]_3$, and extend the series of cyclic $[(2\text{-O-TPP})M^{III}]_3$ complexes to include mixed-metal species. ^{1}H NMR spectroscopy is utilized as a structural probe to identify these new paramagnetic, heterometallic trimers.

Results and Discussion

Molecular Structure of $[(2\text{-O-TTP})Fe^{III}]_3\cdot 3n$-octane. Despite persistent efforts, crystals of cyclic trimers that were suitable for crystallographic study eluded us for several years. Finally we have found a ligand modification and crystallization medium that produced suitable, but small, crystals. Nearly black crystals of $[(2\text{-O-TTP})Fe^{III}]_3\cdot 3n$-octane were obtained by diffusion of *n*-octane into dichloromethane solution of the complex.

Views of the trimeric molecule are shown in Figure 1. Selected interatomic distances and angles are given in Table 1.

The trimer has a cyclic head-to-tail structure with the pyrrolic alkoxide groups forming bridges from one macrocycle to the iron in the adjacent macrocycle. The molecular packing places the axis of the Fe_3 triangle along the crystallographic a direction as shown in Figure 2 which presents the arrangements of the components in three dimensions. The molecules of *n*-octane efficiently fill space between some of the trimeric molecules.

The iron(III) central ions are located at corners of the approximately equilateral triangle at the distance ca. 7 Å (Fe-

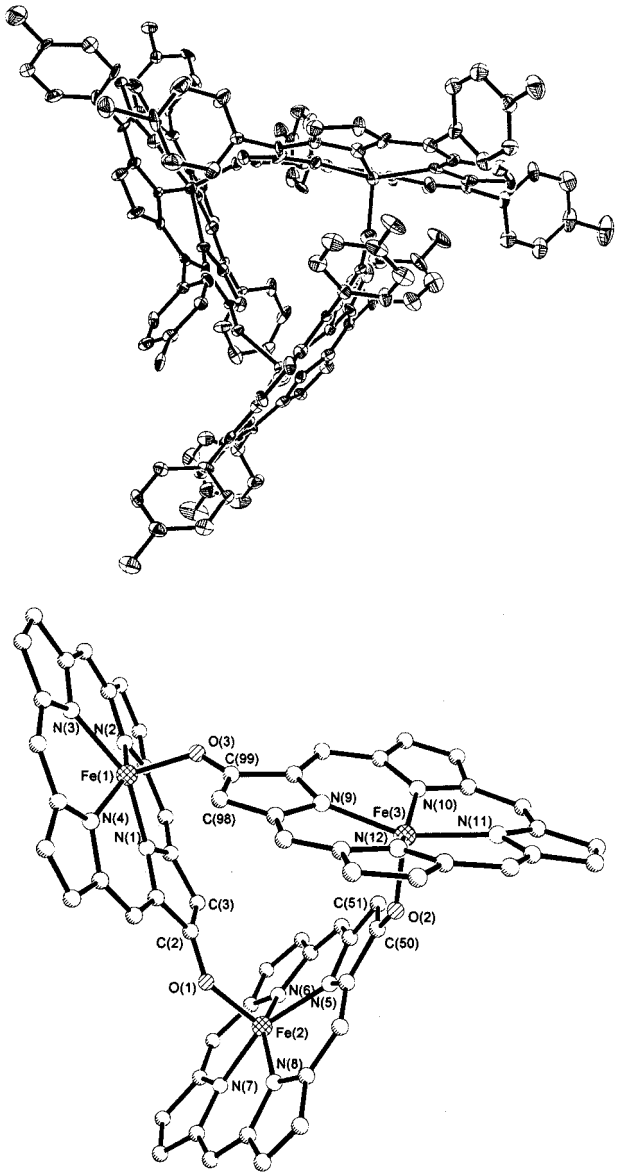

Figure 1. Perspective view of $[(2\text{-O-TTP})Fe^{III}]_3$ with 20% thermal contours. The lower view, in which the aryl groups are omitted, presents the trimer skeleton. The numbering of the porphyrin atoms is sequential, but for clarity only selected atoms are numbered.

(1)−Fe(2), 7.112 Å; Fe(2)−Fe(3), 6.963 Å; Fe(3)−Fe(1), 7.142 Å). The macrocyclic ligands are located in three different planes which form the following dihedral angles: (2-O-TTP)Fe(1)−(2-O-TTP)Fe(2) 65.6°; (2-O-TTP)Fe(2)−(2-O-TTP)Fe(3) 59.3°; (2-O-TTP)Fe(1)−(2-O-TTP)Fe(3) 56.5°.

The smallest interporphyrin contacts are in the range observed in the structures of other metalloporphyrins.[9−12] For example, the 3-H protons are typically located at 2.6−3.0 Å distances from the nearest pyrrole atoms of the neighboring porphyrinic subunit.

In each subunit of the trimer the iron(III) has five-coordinate geometry, and its structural features are consistent with those found for other high-spin five-coordinate iron(III) porphyrin

(9) Scheidt, W. R., Lee, Y. J. *Struct. Bond.* **1987**, *64*, 1.
(10) Balch, A. L.; Noll, B. C.; Olmstead, M. M.; Reid, S. M. *J. Chem. Soc., Chem. Commun.* **1993**, *32*, 1088.
(11) Goff, H. M.; Shimomura, E. T.; Lee, Y. J.; Scheidt, W. R. *Inorg. Chem.* **1984**, *23*, 315.
(12) (a) Wysłouch, A.; Latos-Grażyński, L.; Grzeszczuk, M.; Drabent, K.; Bartczak, T. *J. Chem. Soc., Chem. Commun.* **1988**, 1377. (b) Bartczak, T. J.; Latos-Grażyński, L.; Wysłouch, A. *Inorg. Chim. Acta* **1990**, *171*, 205.

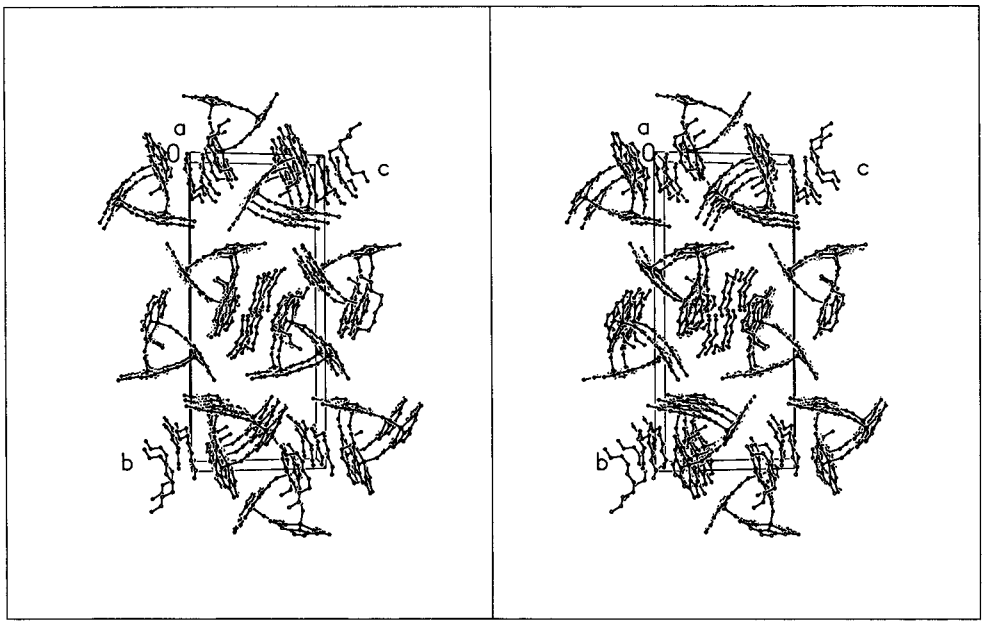

Figure 2. View of the molecular packing in $[(2\text{-O-TTP})Fe^{III}]_3 \cdot 3n\text{-}C_8H_{18}$. For clarity the *p*-tolyl substituents on the porphyrins have been omitted.

Table 1. Selected Bond Lengths and Angles for $[(2\text{-O-TTP})Fe^{III}]_3$

		Bond Lengths (Å)			
Fe(1)−N(1)	2.048(11)	Fe(2)−N(5)	2.073(13)	Fe(3)−N(9)	2.050(13)
Fe(1)−N(2)	2.060(13)	Fe(2)−N(6)	2.049(12)	Fe(3)−N(10)	1.979(13)
Fe(1)−N(3)	2.068(13)	Fe(2)−N(7)	2.077(12)	Fe(3)−N(11)	2.094(13)
Fe(1)−N(4)	2.022(13)	Fe(2)−N(8)	2.036(12)	Fe(3)−N(12)	2.058(12)
Fe(1)−O(3)	1.886(10)	Fe(2)−O(1)	1.873(9)	Fe(3)−O(2)	1.884(10)
		Bond Angles (deg)			
N(1)−Fe(1)−N(3)	154.4(5)	N(5)−Fe(2)−N(7)	157.9(4)	N(9)−Fe(3)−N(11)	156.5(5)
N(2)−Fe(1)−N(4)	151.4(5)	N(6)−Fe(2)−N(8)	153.4(4)	N(10)−Fe(3)−N(12)	152.8(4)

complexes. The average Fe−N distance (2.051 Å) is in the range 2.06(3)−2.087(7) Å expected for this class of molecule.[9,13−21] The iron atoms sit above the mean porphyrin planes with the following out-of-plane displacements: Fe(1), 0.54 Å; Fe(2), 0.43 Å; Fe(3), 0.52 Å. The displacement values are in the expected range observed previously.[9,11−20] Likewise the Fe−O distances (1.886, 1.873, 1.884 Å) are similar to the distances 1.8155(15) Å found in $(TPP)Fe(OCH_3)$[17] and 1.91(2) Å in $[(OEB)Fe^{III}]_2$.[22]

The macrocyclic cores of subunits are far from being planar, and the mean deviations from the macrocycle planes are equal: 0.1232, 0.1545, and 0.1445 Å, respectively. Figure 3 gives out of plane displacements from the mean porphyrin plane for the atoms of the porphyrin core in the three subunits of $(2\text{-O-TTP})Fe^{III}$. The configuration of the porphyrin macrocycle can be described as both saddle-shaped and appreciably ruffled.[9] The dihedral angles of the phenyl ring planes with respect to the macrocycle plane of the adjoining subunit are in the range 56.0−89.6°. These values are in the 50−90° range of dihedral angles observed for crowded diiron tetraarylporphyrins: $[(TPP)Fe^{III}]_2SO_4$,[18] $[(TPP)Fe^{III})]_2O$,[19] $[(TPP)Fe]_2N$,[23] $[(Fe^{III}\text{-}\mu\text{-}O)FF\cdot H_2O]$,[20] $[(TPP)Fe^{III}OFe^{III}(NCH_3TPP)]ClO_4$.[12]

Figure 4 shows a space-filling drawing of the porphyrin core in $[(2\text{-O-TTP})Fe^{III}]_3$ with van der Waals contours represented. There is a significant void at the center of the molecule and no untoward contacts between the components that make up the trimer. In spite of the molecular restrictions necessary to accommodate this trimeric geometry, a rather moderate adjustment of $(TTP)Fe^{III}X$ geometry via folding of the macrocycle core and rotation of the *meso*-phenyl positions has been sufficient to satisfy the steric requirements imposed by the trimer. Such modifications fit in the general picture of the macrocycle flexibility observed for a large variety of high-spin iron porphyrins.[9−24]

It is noteworthy that the structural features seen in the previous molecular mechanics calculations for $[(2\text{-O-TPP})Fe^{III}]_3$ and $[(2\text{-O-TPP})Ga^{III}]_3$ are borne out in the structural study of $[(2\text{-O-TTP})Fe^{III}]_3$. We point out that molecular mechanics analysis respected the well-defined geometric restraints on interporphyrin contacts between all subunits of the trimer derived from ^1H NMR two-dimensional NOESY studies. In particular, a determination of NOE connectivities of $[(2\text{-O-TPP})Ga^{III}]_3$ subunits provided even the very fine details of the structure including localization of the phenyl rings.[5] Although qualitative

(13) (a) Hoard, J. L.; Cohen, G. H.; Glick, M. D. *J. Am. Chem. Soc.* **1967**, *89*, 1992. (b) Scheidt, W. R.; Finnegan, M. G. *Acta Crystallogr.* **1989**, *C45*, 1214.
(14) Hatano, K.; Scheidt, W. R. *Inorg. Chem.* **1979**, *18*, 877.
(15) Skelton, B. W.; White, A. H. *Aust. J. Chem.* **1977**, *30*, 2655.
(16) Phillippi, M. A.; Baenziger, N.; Goff, H. M. *Inorg. Chem.* **1981**, *20*, 3904.
(17) Lecomte, C.; Chadwick, D. L.; Coppens, P.; Stevens, E. D. *Inorg. Chem.* **1983**, *22*, 2982.
(18) Scheidt, W. R.; Lee, Y. J.; Bartczak, T.; Hatano, K. *Inorg. Chem.* **1984**, *23*, 2252.
(19) Hoffman, A. B.; Collins, D. M.; Day, V. W.; Fleischer, E. B.; Srivastava, T. S.; Hoard, J. L. *J. Am. Chem. Soc.* **1972**, *94*, 3620.
(20) Landrum, J. T.; Grimmett, D.; Haller, K. J.; Scheidt, W. R.; Reed, C. A. *J. Am. Chem. Soc.* **1981**, *103*, 2640.
(21) Grinstaff, M. W.; Hill, M. G.; Birnbaum, E. R.; Schaefer, W. P.; Labinger, J. A.; Gray, H. B. *Inorg. Chem.* **1995**, *34*, 4896.
(22) Balch, A. L.; Latos-Grażyński, L.; Noll, B. C.; Olmstead, M. M.; Safari, N. *J. Am. Chem. Soc.* **1993**, *115*, 9056.
(23) Scheidt, W. R.; Summerville, D. A. Cohen, I. A. *J. Am. Chem. Soc.* **1976**, *98*, 6623.
(24) Małek, A.; Latos-Grażyński, L.; Bartczak, T. J.; Żądło, A. *Inorg. Chem.* **1991**, *30*, 3222.

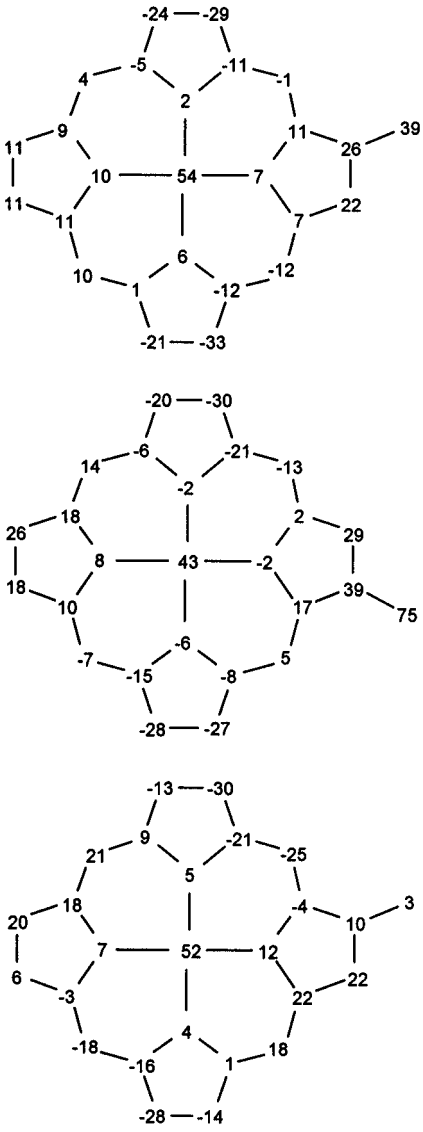

Figure 3. Diagrams of three macrocyclic cores within [(2-O-TTP)-Fe^{III}]$_3$. In each drawing each atom symbol has been replaced by a number representing the perpendicular displacement (in units of 0.01 Å) from the mean plane of the respective cores. The numbers are given successively for Fe(1), Fe(2), and Fe(3) porphyrinic rings.

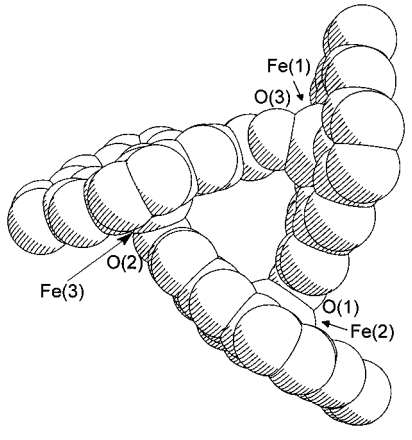

Figure 4. View of the cyclic core of [(2-O-TTP)Fe^{III}]$_3$ with van der Waals contours for all atoms. The *p*-tolyl groups have been omitted.

in its nature, structural information derived from ^{1}H NMR has been fully confirmed by X-ray crystallography.

Synthesis of Heterometallic Trimers. In order to generate cyclic trimers the β-hydroxy derivatives (2-OH-TPP)M^{III}Cl (M = Fe^{III}, Ga^{III}, Mn^{III}) were prepared by a route that involves benzoyloxation of tetraphenylporphyrin, followed by the chromatographic separation of the product and metal insertion to 2-benzoyloxy-TPPH_2.[4−6,8] Ethanolysis of (2-BzO-TPP)M^{III}Cl resulted in formation of the trimeric compounds [(2-O-TPP)-M^{III}]$_3$, which were converted to the respective monomeric (2-OH-TPP)M^{III}Cl complexes by treatment with HCl.[4−6,8] The equimolar mixture of (2-OH-TPP)M^{III}Cl and (2-OH-TPP)-$M_1{}^{III}$Cl was then passed through potassium carbonate and basic alumina to produce a mixture of the heterometallic trimeric molecules. Considering the stoichiometry of the trimer, a set of four different trimeric complexes, {[(2-O-TPP)M^{III})$_n$(2-O-TPP)$M_1{}^{III}$)$_{3-n}$]} (n = 0, 1, 2, 3) should be formed simultaneously. In addition we have attempted to generate [(2-O-TPP)Fe^{III})(2-O-TPP)Ga^{III})(2-O-TPP)Mn^{III})]; i.e., the species where each metal center is different. In this case a mixture of (2-OH-TPP)Fe^{III}Cl, (2-OH-TPP)Ga^{III}Cl, and (2-OH-TPP)-Mn^{III}Cl was subjected to simultanous deprotonation.

Assuming a structure similar to that for the homometallic trimers,[4−6] eight enantiomeric pairs of trimeric species are expected to be formed for each dimetallic system. Twenty-seven enatiomeric pairs can be prepared in a one-pot procedure in the course of the Fe^{III}−Ga^{III}−Mn^{III} oligomerization. In each case attempts to separate these mixtures of trimers through standard column chromatography on alumina or silica gel resulted solely in purification of the trimeric products from the accompanying monomeric species. Thus we have decided to verify their formation using the combination of ^{1}H NMR and mass spectra.

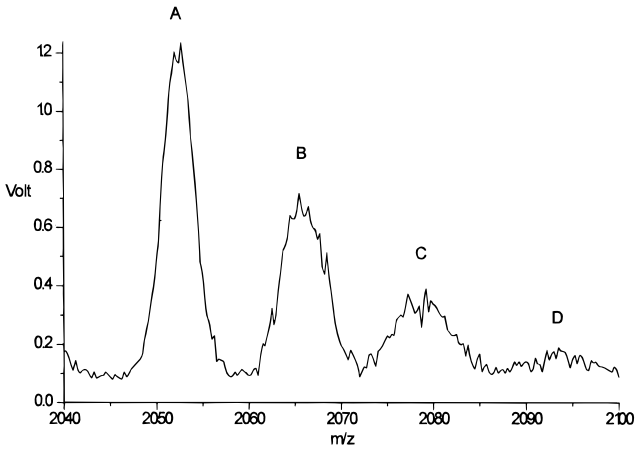

Figure 5. Liquid matrix secondary ion mass spectrum of the [(2-O-TPP)Fe^{III}]$_n$ [(2-O-TPP)Ga^{III}]$_{3-n}$ mixture. The groups of peaks for four different trimetallic complexes are marked separately: (A) [(2-O-TPP)-Fe^{III}]$_3$; (B) {[(2-O-TPP)Fe^{III}]$_2$[(2-O-TPP)Ga^{III}]}; (C) {[(2-O-TPP)Fe^{III}]-[(2-O-TPP)Ga^{III}]$_2$}; (D) residual [(2-O-TPP)Ga^{III}]$_3$.

Mass Spectrometric Studies. A representative mass spectrum is shown in Figure 5. The liquid matrix secondary ion mass spectrum of the {[(2-O-TPP)Fe^{III}]$_n$[(2-O-TPP)Ga^{III}]$_{3-n}$ mixture shows peaks due to the parental species [(2-O-TPP)-Fe^{III}]$_3$ at $(m + 1)/z$ = 2051 (2.5%) and [(2-O-TPP)Ga^{III}]$_3$ at $(m + 1)/z$ = 2092 (traces), mixed complexes {[(2-O-TPP)Ga^{III}]$_2$-[(2-O-TPP)Fe^{III}]} at $(m + 1)/z$ = 2065 (1.5%), and {[(2-O-TPP)Fe^{III}][(2-O-TPP)Ga^{III}]$_2$} at $(m + 1)/z$ = 2079 (0.7%). MS spectra of {[(2-O-TPP)Fe^{III}]$_n$[(2-O-TPP)Ga^{III}]$_{3-n}$} or {[(2-O-TPP)Mn^{III}]$_n$[(2-O-TPP)Ga^{III}]$_{3-n}$} systems obtained with the ESI method also show the presence of heterometallic cyclic trimers. In this technique the peaks of linear trimers of the general formula of {[(2-O-TPP)M^{III}][(2-O-TPP)M^{III}][(2-O-TPP)M^{III}-(OH)} are visible as well. Small differences of atomic masses between Fe and Mn render this approach less analytically useful for unambiguous identification of [(2-O-TPP)Fe^{III})$_n$(2-O-TPP)-

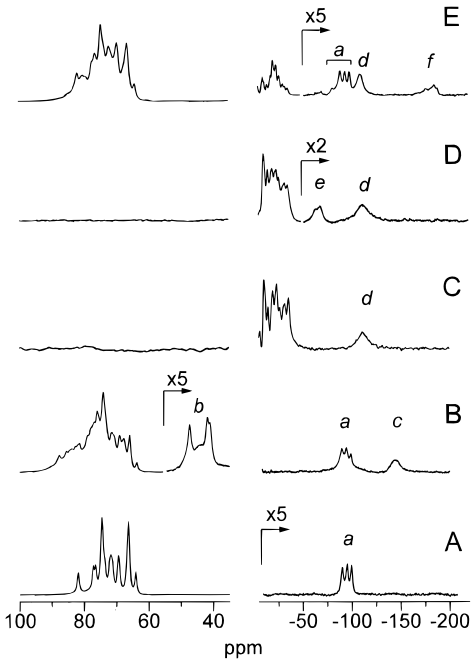

Figure 6. Pyrrole regions of the 300 MHz ^{1}H NMR spectra of mixtures of trimetallic complexes in chloroform-*d* at 293 K. The spectra have been obtained using the inversion−recovery technique. Key: (A) [(2-O-TPP)Fe^{III}]$_3$; (B) [(2-O-TPP)Fe^{III}]$_n$[(2-O-TPP)Ga^{III}]$_{3-n}$; (C) [(2-O-TPP)Mn^{III}]$_3$; (D) [(2-O-TPP)Mn^{III}]$_n$[(2-O-TPP)Ga^{III}]$_{3-n}$; (E) [(2-O-TPP)Fe^{III}]$_n$[(2-O-TPP)Mn^{III}]$_{3-n}$. Only the "fingerprint" 3-H resonances of the trimetallic species are marked as follows: *a*, PFe−O**P**Fe; *b*, PGa−O**P**Fe; *c*, PFe−O**P**Ga; *d*, PMn−O**P**Mn; *e*, PMn−O**P**Ga, PGa−O**P**Mn; *f*, PMn−O**P**Fe.

Table 2. ^{1}H NMR Chemical Shifts for 3-H Pyrrole Protons of [(2-O-TPP)M^{III}]$_n$[(2-O-TPP)M$_1^{III}$]$_{3-n}$ Compounds[a]

compds	δ (ppm)	ref
[(2-O-TPP)Fe^{III}]$_3$	−89.8, −94.7, −99.3	4
[(2-O-TTP)Fe^{III}]$_3$	−88.6, −92.7, −98.3	*i*
[(2-O-TPP)Mn^{III}]$_3$	−111.5	6
[(2-O-TPP)Ga^{III}]$_3$[b]	1.82, 2.18, 2.82	5
[(2-O-TPP)Fe^{III}]$_2$[(2-O-TPP)Ga^{III}]	−145;[c] 41,[d] 42,[d] 47[d]	*i*
[(2-O-TPP)Ga^{III}]$_2$[(2-O-TPP)Fe^{III}]	−145,[c] 44[d]	*i*
[(2-O-TPP)Mn^{III}]$_n$[(2-O-TPP)Ga^{III}]$_{3-n}$	−65,[e] −70[f]	*i*
[(2-O-TPP)Mn^{III}]$_n$[(2-O-TPP)Fe^{III}]$_{3-n}$	−175,[g] −185,[g] −190;[g] −80[h]	*i*

[a] The spectra obtained in chloroform-*d* at 291−293 K unless marked differently. [b] 243 K. [c] PFe−O**P**Ga. [d] PGa−O**P**Fe. [e] PMn−O**P**Ga. [f] PGa−O**P**Mn. [g] PFe−O**P**Mn. [h] PFe−O**P**Fe in [(2-O-TPP)Mn^{III}][(2-O-TPP)-Fe^{III}]$_2$. [i] This work.

Mn^{III})$_{3-n}$] or {[(2-O-TPP)Fe^{III}][(2-O-TPP)Mn^{III})][(2-O-TPP)-Ga^{III})]} in the complex reaction mixture.

^{1}H NMR Identification of Heterometallic Trimers. The ^{1}H NMR spectra obtained for products of (2-O-TPP)Fe^{III}−(2-O-TPP)Ga^{III}, (2-O-TPP)Mn^{III}−(2-O-TPP)Ga^{III}, and (2-O-TPP)-Fe^{III}−(2-O-TPP)Mn^{III} oligomerizations are collected in Figure 6. The relevant values of chemical shifts are gathered in Table 2.

Considering the intrinsic asymmetry of the *RRS* (*SSR*) cyclic trimer framework, the following species can be formed when two building blocks, (2-OH-TPP)M^{III} and (2-OH-TPP)M$_1^{III}$, are considered: *R*(M)*R*(M)*S*(M), *R*(M$_1$)*R*(M)*S*(M), *R*(M)*R*(M$_1$)-*S*(M), *R*(M)*R*(M)*S*(M$_1$), *R*(M$_1$)*R*(M$_1$)*S*(M), *R*(M)*R*(M$_1$)*S*(M$_1$), *R*(M$_1$)*R*(M)*S*(M$_1$), and *R*(M$_1$)*R*(M$_1$)*S*(M$_1$) and their respective enantiomers *S*(M)*S*(M)*R*(M), *S*(M$_1$)*S*(M)*R*(M), *S*(M)*S*(M$_1$)*R*(M), *S*(M)*S*(M)*R*(M$_1$), *S*(M$_1$)*S*(M$_1$)*R*(M), *S*(M)*S*(M$_1$)*R*(M$_1$), *S*(M$_1$)-*S*(M)*R*(M$_1$), *S*(M$_1$)*S*(M$_1$)*R*(M$_1$). The *RRS* and *SSR* enantiomeric pairs are indistinguishable by means of ^{1}H NMR in conventional achiral environments. Taking into account the multiplicity and similarity of the cyclic trimers, the task of the trimer detection is analytically demanding. At the present stage of the project we limited ourselves to spectroscopic identification of heterometallic trimers.

Accordingly we have noticed that only the 3-H resonance offers a chance to get an insight into the mixed trimer formation as the corresponding resonances are located in suitable, well-separated spectral regions. Their paramagnetic shifts reflect simultaneously contributions of two neighboring metal centers. The remaining paramagnetically shifted pyrrolic resonances reveal barely resolved clusters of 72 strongly overlapped lines. For instance, considering solely the (2-O-TPP)M^{III} moiety, the total number of the inequivalent components in the region of its 7,8,12,13,17,18-H resonances equals 72 (*R*(M)*R*(M)*S*(M), 18; *R*(M$_1$)*R*(M)*S*(M), 12; *R*(M)*R*(M$_1$)*S*(M), 12; *R*(M)*R*(M)*S*(M$_1$), 12; *R*(M$_1$)*R*(M$_1$)*S*(M), 6; *R*(M)*R*(M$_1$)*S*(M$_1$), 6; *R*(M$_1$)*R*(M)*S*(M$_1$), 6; *R*(M$_1$)*R*(M$_1$)*S*(M$_1$), 0). These protons are sufficiently isolated from the influence of other paramagnetic centers. Therefore, their resonances are located in regions which are typical for the respective monomeric metalloporphyrin (2-O-TPP)M^{III}, although some modifications of paramagnetic shifts have been noticed.

The representative spectroscopic analysis is presented in detail for the (2-O-TPP)Ga^{III}−(2-O-TPP)Fe^{III} experiment. The β-hydroxyporphyrin of each monomeric unit is coordinated simultaneously to the internal metal(III) through four nitrogen atoms and to the external one by the oxygen atom. The formation of the mixed iron(III)−gallium(III) trimer creates the following environment of 3-H in the single trimeric units:

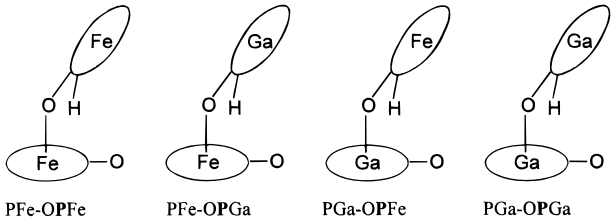

Effectively, the presence of the diamagnetic gallium(III) dilutes paramagnetic centers in {[(2-O-TPP)Ga^{III}][(2-O-TPP)Fe^{III}]$_2$} and {[(2-O-TPP)Ga^{III}]$_2$[(2-O-TPP)Fe^{III}]}with respect to [(2-O-TPP)-Fe^{III}]$_3$ and produces well-separated contributions of external and internal coordinated iron(III) to the resultant paramagnetic shift of the 3-H resonances. As expected, PFe−O**P**Fe and PGa−O**P**Ga elements contribute to the spectrum in the regions which are typical for the homometallic trimers.[4−6]

The very broad, unresolved group at −145 ppm is readily identified and is assigned to 3-H resonances of PFe−O−**P**Ga type fragments in the following trimers: *R(Fe)R(Ga)*S(Ga), R(Ga)*R(Fe)S(Ga)*, *R(Ga)*R(Ga)*S(Fe)*, R(Fe)*R(Fe)S(Ga)*, *R-(Fe)R(Ga)*S(Fe), *R(Ga)*R(Fe)*S(Fe)* (Figure 6, trace B). A new multiplet centered at 45 ppm shows three narrower resonances siting on a top of a much broader feature. We have applied the deconvolution procedure to demonstrate that three narrower lines have similar line width (ca. 250 Hz). Following symmetry considerations, the broader (ca. 1650 Hz) part is presumably also composed of three similar but broader lines. Assuming the narrowest limit for three 3-H components, the line widths for these three have been estimated to be one-third of the entire resonance (i.e. 550 Hz) which is definitely much larger than that for three other pyrrole resonances in this region. We have assigned the three narrower lines to the PGa−O−**P**Fe element built into diiron−monogallium trimers *R(Fe)*R(Fe)*S(Ga)*, R(Fe)-*R(Ga)S(Fe)*, and *R(Ga)R(Fe)*S(Fe). As expected, {[(2-O-TPP)-Ga^{III}]$_2$[(2-O-TPP)Fe^{III}]} reveals features of the diamagnetically diluted [(2-O-TPP)Fe^{III}O] species affording the broad 3-H

resonance usually expected for iron(III) high-spin porphyrins with oxygen in the axial position.[4] As a matter of fact the position of the 3-H resonances determined for the PFe−O−**P**Ga fragment resembles quite well the characteristic values established previously for the relevant high-spin complexes: [(2-O-TPP)Fe^{III}(OH)]$^-$ (33.4 ppm), [(2-O-TPP)Fe^{III}(OCH_3)]$^-$ (33.7 ppm).[4] The coordination of gallium(III) slightly perturbs the electronic structure of the [(2-O-TPP)Fe^{III} unit producing a *ca*. 10 ppm downfield modification. The effect of protonation is remarkably larger since (2-OH-TPP)Fe^{III}Cl has the 3-H resonance at 79.1 ppm (all values given at 293 K). In general, line widths of [(2-O-TPP)Fe^{III}]$_3$ and {[(2-O-TPP)Fe^{III}]$_2$[(2-O-TPP)-Ga^{III}]} resonances are markedly smaller than those determined for {[(2-O-TPP)Ga^{III}]$_2$[(2-O-TPP)Fe^{III}]} and corresponding monomeric species.[4,6] This rather general phenomenon usually reflects some interaction between closely related paramagnetic centers. This interaction decreases the T_{1e} relaxation time and produces a narrowing of ^{1}H NMR resonances.[25] In light of this analysis, it is clear that only {[(2-O-TPP)Ga^{III}]$_2$[(2-O-TPP)Fe^{III}]} presents a well-defined EPR spectrum typical for monomeric high-spin iron porphyrins with $g_\perp = 6$ and $g_\parallel = 2$ where the diiron and triiron species are EPR silent.[4]

Using a similar approach as presented above, we have tentativety identified the resonances of the characteristic fragments for the Mn^{III}−Ga^{III} pair as shown in Figure 6 and Table 2.

Finally we have embarked on the most complicated situation, i.e. the Mn^{III}−Fe^{III} pair where both metal ions produce paramagnetic shifts. We could easily identify enormously shifted set of resonances at ca. −200 ppm assigned to PFe^{III}−O**P**Mn^{III} fragments of {[(2-O-TPP)Mn^{III}][(2-O-TPP)Fe^{III}]$_2$} and {[(2-O-TPP)Mn^{III}]$_2$[(2-O-TPP)Fe^{III}]}. The unidentified 3-H resonances of PMn^{III}−O−**P**Fe^{III} are probably located in the crowded region of manganese pyrrolic resonances (*vide infra*).

Assuming the simple additivity, we have previously evaluated the external and internal contribution to the paramagnetic shifts of the 3-H resonances for [(2-O-TPP)Mn^{III}]$_3$ and [(2-O-TPP)-Fe^{III}]$_3$ although the relevant isolated contributions of two paramagnetic centers were not accessible.[4,6]

Here we have searched for better founded, relevant increments of the paramagnetic shift resulting from the internal and external interactions. In principle they can be determined for the appropriate motifs of {[(2-O-TPP)Ga^{III}]$_n$[(2-O-TPP)Fe^{III}]$_{3-n}$} and {[(2-O-TPP)Ga^{III}]$_n$[(2-O-TPP)Mn^{III}]$_{3-n}$} structures, respectively. Thus we have elucidated directly the following 3-H shift increments as equal to isotropic shifts of listed fragments: PFe−O**P**Ga, −145 ± 5 ppm; PGa−O**P**Fe, 45 ± 5 ppm; PMn−O**P**Ga, −65 ± 10 ppm; PGa−O**P**Mn, −70 ± 10 ppm. In the case of the multiplet structure, the center of the group is given. The spread of resonances is reflected by the range of expected values.

The chemical shifts can be estimated for the following pairs: PFe−O**P**Fe = PGa−O**P**Ga + PFe−O**P**Ga + PGa−O**P**Fe, −98 ppm ± 10 ppm; PMn−O**P**Mn = PGa−O**P**Ga + PMn−O**P**Ga + PGa−O**P**Mn, −133 ± 20 ppm; PFe−O**P**Mn = PGa−O**P**Ga + PFe−O**P**Ga + PGa−O**P**Mn, −213 ± 15 ppm; PMn−O**P**Fe = PGa−O**P**Ga + PMn−O**P**Ga + PGa−O**P**Fe, −18 ± 15 ppm (PGa−O**P**Ga ≈ 2 ppm).[5]

The first three values are significantly consistent with the observed shifts for the corresponding Mn^{III}−Fe^{III} cyclic complexes (Table 2), and the fourth value allows one to locate tentatively the 3-H missing resonance of PMn−O**P**Fe in the crowded 0 to −40 ppm spectral region.

In order to complete the picture we attempted to assemble three different starting blocks simultaneously. The generated spectra demonstrate the overlay of features generated in three independent experiments: (2-OH-TPP)Fe^{III} and (2-OH-TPP)-Ga^{III}, (2-OH-TPP)Mn^{III} and (2-OH-TPP)Ga^{III}, (2-OH-TPP)Mn^{III} and (2-OH-TPP)Fe^{III}. The expected patterns of the six isomeric forms *R*(Fe)*R*(Ga)*S*(Mn), *R*(Fe)*R*(Mn)*S*(Ga), *R*(Ga)*R*(Mn)*S*(Fe), *R*(Ga)*R*(Fe)*S*(Mn) *R*(Mn)*R*(Fe)*S*(Ga), and *R*(Mn)*R*(Ga)*S*(Fe) may add to the spectral complexity. However, according to our shift analysis all resonances of Ga−Fe−Mn complexes will be eventually located in the region previously determined for a simple binary system and therefore escape an unambiguous identification.

Table 3. Crystallographic Data for [(2-O-TTP)Fe^{III}]$_3$·3*n*-octane

empirical formula	$C_{168}H_{159}Fe_3N_{12}O_3$
color, habit	black needles
fw	2651.62
cryst system	monoclinic
space group	$P2_1/n$
unit cell dimens	$a = 16.729(6)$ Å, $\alpha = 90°$; $b = 43.671(13)$ Å, $\beta = 105.83(3)°$; $c = 19.564(7)$ Å, $\gamma = 90°$
V	13751(8) Å^3
T	130(2) K
Z	4
cryst size	0.36 × 0.10 × 0.02 mm
d_{calcd}	1.273 Mg/m^3
radiation λ	1.541 78 Å (Cu Kα)
μ(Cu Kα)	2.973 mm^{-1}
range of transm factors	0.96−0.78
R_1[a]	0.089
wR_2[b]	0.1848

[a] $R_1 = \sum||F_o| - |F_c||/\sum|F_o|$. [b] $wR_2 = [\sum[w(F_o^2 - F_c^2)^2]/\sum[w(F_o^2)^2]]^{1/2}$.

Exchange Reaction between Intact Trimers. With the heterotrinuclear complexes spectroscopically detected in the preceding work, it was also possible to look for the formation of such species for the scrambling reaction of intact trimers. Analysis of an equimolar mixture of [(2-O-TPP)Fe^{III}]$_3$ and [(2-O-TPP)Ga^{III}]$_3$ in chloroform-*d* by ^{1}H NMR spectroscopy showed no traces of heterometallic trimers even after several weeks or when subjected to chromatography on silica or basic alumina. Thus the trimeric units are stable with respect to interchange of individual monoporphyrinic units.

Conclusion

The X-ray crystallographic investigation of [(2-O-TTP)Fe^{III}]$_3$ has confirmed the previous ^{1}H NMR structural data that indicated that these molecules formed cyclic trimers with the *RRS*/*SSR* structure (**2**). In our previous investigation of paramagnetic iron(III) and manganese(III) and diamagnetic gallium(III) complexes we have determined diagnostic ^{1}H NMR resonances for the cyclic trimer formation in the self-assembly process from monomeric monomeric iron(III) 2-hydroxytetraphenylporphyrin, manganese(III) 2-hydroxytetraphenylporphyrin, or gallium(III) 2-hydroxytetraphenylporphyrin building blocks. In this paper we have found that the compatibility of [(2-O-TPP)M^{III}] fragments affords the construction of heterometallic complexes that preserve the general framework of [(2-O-TTP)Fe^{III}]$_3$. The 3-H resonances offer a distinct characteristic for these heterometallic paramagnetic complexes.

Experimental Section

Solvents and Reagents. All solvents were purified by standard procedures. Chloroform-*d* ($CDCl_3$, Glaser AG) was dried before use by passing through activated basic alumina.

Preparation of Compounds. (2-OH-TPP)Fe^{III}Cl, (2-OH-TPP)Mn^{III}-Cl, (2-OH-TPP)Ga^{III}Cl, [(2-O-TPP)Fe^{III}]$_3$, [(2-O-TPP)Mn^{III}]$_3$, and [(2-O-TPP)Ga^{III}]$_3$ were prepared as described previously.[4−6] [(2-O-TTP)-Fe^{III}]$_3$ was obtained in a manner analogous to [(2-O-TPP)Fe^{III}]$_3$.[4]

(25) Bertini, I.; Luchinat, C. *Coord. Chem. Rev.* **1996**, *150*, 131.

{[(2-O-TPP)M_1^{III}]$_n$[(2-O-TPP)M_1^{III}]$_{3-n}$}. (2-OH-TPP)M^{III}Cl (5 mg) and (2-OH-TPP)M_1^{III}Cl (5 mg) were dissolved in dichloromethane and passed through a basic alumina column with a layer of solid potassium carbonate. Elution with dichloromethane/methanol (98/2 v/v) gave the usually brown fraction that was recovered as the solvent was removed under vacuum. The sample was used in ^{1}H NMR investigations.

Instrumentation. ^{1}H NMR spectra were recorded on a Bruker AMX spectrometer operating in the quadrature mode at 300 MHz. A typical spectrum was collected over a 60 000−90 000 Hz spectral window with 16 K data points with 500−5000 transients for the experiment and a 50 ms prepulse delay. The free induction decay (FID) was apodized using exponential multiplication depending on the natural line width. This induced 5−100 Hz broadening. The residual ^{1}H NMR resonances of the deuterated solvents were used as a secondary reference. An inversion−recovery sequence was used to suppress the diamagnetic signals in the selected spectra. Mass spectra were recorded on a ADM-604 spectrometer using the liquid matrix secondary ion mass spectrometry technique and a primary beam of 8 keV Cs^+ ions and on a Finnigan TSQ 700 spectrometer equipped with an ESI ion source operating at 4.5 kV.

EPR spectra were recorded on a Bruker ESP 300 E spectrometer equipped with a Hewlett-Packard 5350 B frequency counter.

X-ray Structure Determination. X-ray Data Collection. Crystals of [(2-O-TTP)Fe^{III}]$_3$·3*n*-octane were prepared by diffusion of *n*-octane into a dichloromethane solution of the complex in a thin tube. A suitable crystal was coated with the light hydrocarbon oil and directly mounted in the 130 K dinitrogen stream of the low-temperature apparatus. Data were collected at 130 K on a Siemens P4/RA diffractometer that was equipped with a Siemens LT-2 low-temperature apparatus. Two check reflections showed random (less than 2%) variation during the data collection. The data were corrected for Lorentz and polarization effects. The radiation employed was Ni-filtered Cu Kα from a Siemens rotating anode source operating at 15 kW. Crystal data are compiled in Table 3.

Solution and Structure Refinement. Calculations were performed on a PC with programs of SHELXTL v.5. Scattering factors for neutral atoms and corrections for anomalous dispersion were taken from a standard source.[26] The solutions were obtained by Patterson methods. Three molecules of *n*-octane in the lattice exhibit disorder. Molecule 1 is disordered at the ends; C(143), C(146), C(15A), and C(15B) were refined at 50% occupancy. Sites 2 and 3 have two different molecules in each site and were refined with common thermal parameters and variable occupancies for the two parts. Thus, {C(153)−C(160); C(161)−C(168)} with relative occupancies {0.554(16); 0.446(16)} and *U* of 0.164 Å^2 comprise site 2 while {C(169)−C(176); C(177)−C(184)} with relative occupancies {0.554(14); 0.446(14)} and *U* of 0.154(5) Å^2 comprise site 3. Restraints of 1.54(2) Å for 1−2 distances and 2.52(2) Å for 1−3 distances were applied for the carbon atoms in this molecule during refinement. No hydrogen atoms were included for the molecules of *n*-octane.

Acknowledgment. The financial support of the State Committee for Scientific Research of Poland, KBN (Grant 3 T09A 143 09), and the U.S. National Institutes of Health (Grant GM 26226) is kindly acknowledged.

Supporting Information Available: Tables of crystal data, atom coordinates, complete bond lengths and angles, anisotropic displacement coefficients, and calculated hydrogen parameters (26 pages). Ordering information is given on any current masthead page.

IC970214Q

(26) *International Tables for X-ray Crystallography*; D. Reidel Publishing Co.: Boston, MA, 1991; Vol. C.